

## High-energy *K*-line PIXE spectra of Au-bearing minerals

NORMAN M. HALDEN, FRANK C. HAWTHORNE

Department of Geological Sciences, University of Manitoba, Winnipeg, Manitoba R3T 2N2, Canada

J. J. GUY DUROCHER, GARRY S. SMITH, DAMION M. GALLOP, JASPER S. C. MCKEE

Department of Physics, University of Manitoba, Winnipeg, Manitoba R3T 2N2, Canada

### ABSTRACT

Au-bearing minerals in a sulfide- and a quartz-vein ore have been characterized by 40-MeV proton-induced X-ray emission (PIXE). For samples in which Au is the only heavy element, all four *K* X-ray lines are well-resolved in the energy range of 68–81 keV. When other heavy elements are present (e.g., Hg), *K*-line overlap occurs, but the resolution of all four *K*-line components for each element should allow quantitative relative intensities to be derived. Additional complications can arise from nuclear reactions within a sample. For electrum-bearing ore from Trout Lake, Manitoba, Canada, a discrete  $\gamma$ -ray interference was identified. The minerals and composition of this sample precluded any single-stage nuclear reaction mechanism as an origin for the  $\gamma$ -ray; its production was only compatible with the multistage reaction  $^{64}\text{Zn}(p,\alpha)^{61}\text{Cu}^* \rightarrow ^{61}\text{Cu}_{\text{gs}} + \gamma$ , the Zn being present in sphalerite in the sample. This mechanism was confirmed on Zn foil and sphalerite. Previous evaluations have overestimated the problems associated with  $\gamma$ -ray generation in high-energy particle bombardment of geological materials. A brief comparison of low-energy PIXE, high-energy PIXE, and SXRF indicates that high-energy PIXE (HE-PIXE) should be a useful addition to current methods of heavy-element analysis.

### INTRODUCTION

Chemical analysis of sulfides for such elements as Au, Ag, and the platinum-group elements (PGE) has gained new momentum with the availability and application of PIXE (proton-induced X-ray emission), micro-PIXE, SXRF (synchrotron X-ray fluorescence) and SIMS (secondary-ion mass spectrometry) analytical techniques (Cabri, 1987; Cabri et al., 1985a; Campbell et al., 1987). This thrust stems from the need to understand the physical and chemical parameters that govern the distribution of these elements between (and within) sulfide phases and native alloys, particularly with regard to the optimization of element extraction processes. High-energy PIXE (HE-PIXE) has only recently been applied to geological materials (Durocher et al., 1988). It is a new analytical technique that is in the development stages of instrumentation and application.

The majority of PIXE work on minerals has used 2–5 MeV proton beams for excitation and thick targets (ca. 1 mm) (Cabri et al., 1984, 1985a; Rogers et al., 1984; MacArthur et al., 1987; Waychunas, 1988). Protons of such energies do not efficiently excite *K* lines for high atomic-number elements, and low-energy PIXE (LE-PIXE) normally uses the *L* X-ray series (for heavy-element analysis). The resulting spectra can require stripping techniques to resolve overlap problems (MacArthur et al., 1987).

Until recently, it was thought that PIXE analysis of minerals was restricted to excitation protons in the energy

range of 2–5 MeV (cf. McKee et al., 1990). Review articles by Cookson (1979, 1981) concentrated on the applications of LE-PIXE using SiLi detectors. Gerve and Schatz (1975) suggested that it would be advantageous to keep excitation energies as low as possible to “reduce the number of different nuclear reactions” that might contribute low-energy  $\gamma$ -ray peaks to the spectrum. The occurrence of discrete  $\gamma$ -ray interferences is distinct from problems related to background. It might be expected that high-energy proton bombardment of complex geological materials would produce a large number of nuclear reactions, with the result that low-energy  $\gamma$ -rays from those reactions could interfere with the X-ray spectra of the elements of interest. This is to some extent borne out by the work of Folkmann et al. (1974) who observed peaks in their spectra that they interpreted to be “of nuclear origin.” In this case, the projectiles used were  $\alpha$  particles, and the peaks of nuclear origin were produced when the energy of the  $\alpha$  particles was increased. However, Durocher et al. (1988) reported well-resolved *K*-line spectra for the rare-earth elements (REEs) in several apatites, showing that interference due to low-energy  $\gamma$ -rays from nuclear reactions is not a necessary result of using high-energy protons for excitation.

It has been suggested also that the Compton scattering of  $\gamma$ -rays within the Ge detector might significantly increase the background for experiments run at higher proton energies (ca. 30 MeV), to the extent that this component of the background might effectively obscure *K*

X-ray peaks. McKee et al. (1976) have shown that this is not the case. From the work of Durocher et al. (1988), we see that the *K* lines from a number of elements are clearly resolved with high peak-to-background ratios, and that high levels of bremsstrahlung are not a significant problem. These results are to be expected, as the cross section for *K*-shell ionization of medium- to high-*Z* elements reaches a maximum in the proton energy range of 30–50 MeV (McKee et al., 1976).

Because of the current interest in the distribution of Au in sulfide minerals, it seemed worthwhile to explore the analytical potential of HE-PIXE in this area.

### SAMPLE SELECTION AND PREPARATION

Two Au-bearing ores were selected for analysis. The first sample was a quartz-vein ore from the Cochenour-Willans Au mine, Red Lake, Ontario, Canada; this sample contained arsenopyrite, visible Au, stibnite, and quartz. The other sample was from a massive sulfide deposit at Trout Lake, Manitoba, and contained chalcopyrite, pyrite, minor sphalerite, and electrum (Healy and Petruk, 1988). The samples were initially prepared as ground slabs. These were mounted on glass slides using piccolyte, ground to a thickness of approximately 80  $\mu\text{m}$ , and polished. They were then remounted and polished on the reverse side, the final sections being approximately 30–50  $\mu\text{m}$  thick. The last stage included separation of the sections from the glass slides and washing in xylol. The final product is a self-supporting, doubly-polished rock slice 30–50  $\mu\text{m}$  thick similar to that used in fluid inclusion studies. The thin wafers were then suspended in Mylar envelopes and mounted in Al frames for PIXE analysis. Specimens prepared in this manner also have the advantage of being amenable to a number of other forms of analysis: electron microprobe, fluid inclusion, transmitted and reflected light, and infrared microscopy.

### EXPERIMENTAL METHOD

The target frames were mounted in an evacuated chamber on an experimental beam line at the cyclotron facility at the University of Manitoba Accelerator Centre. There they were exposed to a 40-MeV proton beam, 2 mm in diameter, with an average beam current on target of 10 nA. The energy loss of the beam for targets of this thickness is negligible (<500 keV), and hence it is not necessary to cool the target. After passing through the target, the beam was stopped in a shielded, biased Faraday cup that was continuously monitored. X-rays emitted from the sample were analyzed using an intrinsic Ge detector, and signals were processed using standard NIM and Camac electronics. The detector and electronics were calibrated using a  $^{241}\text{Am}$  source. Data were accumulated and recorded to disk on a VAX 11/750 computer with the data measurement and analysis program XSYS (Gould et al., 1981). Detailed analysis was later done off-line using the same program.

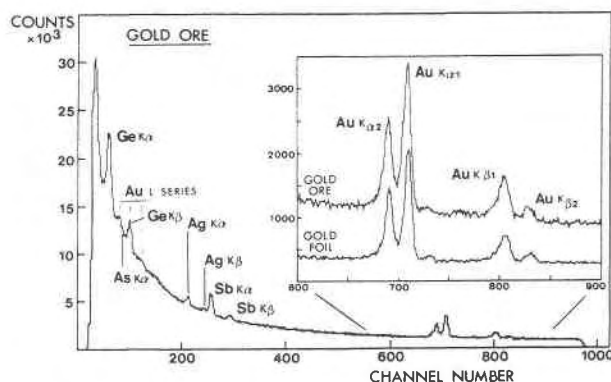


Fig. 1. Observed spectrum of the Cochenour-Willans Au ore sample showing *K* X-ray lines for  $\text{GeK}\alpha$  (9.87 keV) and  $\text{K}\beta$  (10.98 keV);  $\text{GeK}\beta$  overlaps with one of the Au *L*-lines;  $\text{AsK}\alpha$  (10.54 keV); Au *L*-series (between 9.71 and 13.37 keV);  $\text{AgK}\alpha$  and  $\text{K}\beta$  (22.10 and 24.98 keV, respectively);  $\text{SbK}\alpha$  and  $\text{SbK}\beta$  (26.27 and 29.85 keV, respectively) and  $\text{AuK}\alpha_1$ ,  $\text{AuK}\alpha_2$ ,  $\text{AuK}\beta_1$ , and  $\text{AuK}\beta_2$  (68.79, 66.98, 77.96, and 80.16 keV, respectively). The inset spectrum shows an expansion of the region containing the Au lines, and a reference spectrum of Au foil for comparison). The position of the  $\text{AsK}\alpha$  peak was checked against a reference spectrum collected from  $\text{As}_2\text{O}_3$ .

### RESULTS

A raw spectrum from the Cochenour-Willans sample is shown in Figure 1. The spectrum took 20 min to record; note that the plot has linear scales, and without data reduction, it is possible to clearly identify a number of peaks in the 9–90 keV region. At the low-energy end of the spectrum, we see *K* lines for Ge, As, Ag, and Sb, and *L* lines for Au. This is the X-ray energy range normally accessible to LE-PIXE analysis. The Ge X-ray lines are the result of elastic proton scattering from the target, scattered protons causing some excitation in the Ge detector. It should also be noted that this has not contributed to the bremsstrahlung at the high-energy end of the spectrum, where in the 68–81 keV range, a number of significant peaks are observed. These peaks are shown as the upper spectrum in the inset of Figure 1; there are four easily resolved peaks that correspond in energy and relative intensity to the *K*-line series for Au. This identification is confirmed by comparison with the spectrum of Au foil (Fig. 1 inset, lower spectrum). All the Au *K* lines ( $\text{AuK}\alpha_1$ ,  $\text{K}\alpha_2$ ,  $\text{K}\beta_1$ , and  $\text{K}\beta_2$ ; 68.79, 66.98, 77.96, and 80.16 keV respectively) are completely available for analytical purposes in this sample.

Figure 2 is the spectrum recorded from the Trout Lake sample. Comparison of Figure 2 with Figure 1 shows that the former is significantly more complicated in the region of the Au *K* lines. Focusing on Figure 2, we note the following key points: (1) there is an additional peak to the high-energy side of the  $\text{AuK}\alpha$  doublet, and (2) the peaks at the positions of  $\text{AuK}\alpha_1$  and  $\text{AuK}\alpha_2$  do not have the correct relative intensities (Scofield, 1974) to be solely due to Au. The  $\text{AuK}\beta$  doublet is present and can be used

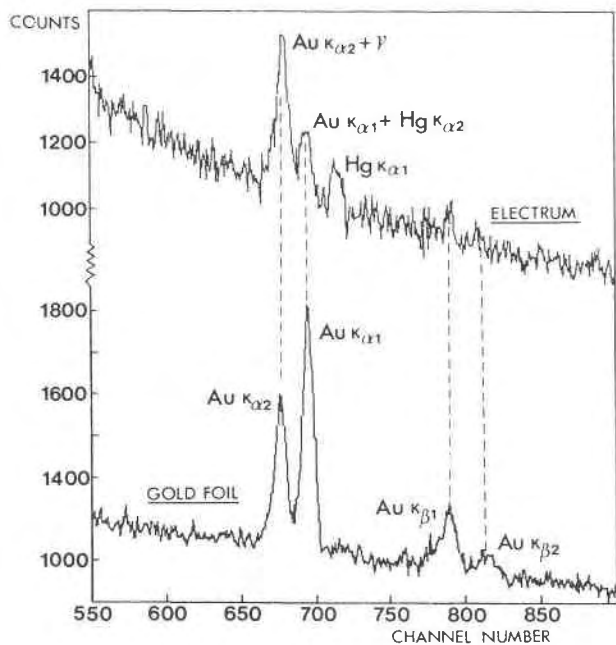


Fig. 2. Spectra taken from the Trout Lake electrum sample and the Au-foil reference. In addition to the Au lines, the spectrum shows the  $HgK_{\alpha 1}$  peak at 70.82 keV and the enhancement of the  $AuK_{\alpha 2}$  peak by a discrete  $\gamma$ -ray at 67 keV.

to provide quantitative analytical data. However, the  $K\beta$  peaks are intrinsically weaker than the  $K\alpha$  peaks, and consequently are not ideal for analytical purposes. It would be better to understand why the  $AuK_{\alpha}$  doublet has an anomalous intensity ratio and to correct the intensities for whatever effects are giving rise to the aberrant ratio.

Considering point 1 above, the principal Au-bearing phase in the sample is electrum, an Au-Ag-Hg alloy. The peak on the high-energy side of the  $AuK_{\alpha 1}$  line corresponds exactly in energy to  $HgK_{\alpha 1}$  and can be thus assigned. This means that there is an  $HgK_{\alpha 2}$  component to the low-energy side of the  $HgK_{\alpha 1}$  peak. The position of this peak corresponds almost exactly with the position of the  $AuK_{\alpha 1}$  peak. Thus in the upper spectrum of Figure 2, the peak corresponding in energy to  $AuK_{\alpha 1}$  (shown in the lower spectrum) is actually a composite peak, owing to overlap of  $AuK_{\alpha 1}$  and  $HgK_{\alpha 2}$ . With reference to point 2, such an overlap should perturb the relative peak intensities of  $AuK_{\alpha 1}$  and  $AuK_{\alpha 2}$  in a manner opposite to what is observed. Hence there must be another contribution to the observed intensity ratio of this doublet. As there are no other X-ray lines observed in this region, we conclude that there must be a discrete  $\gamma$ -ray contributing to the spectrum at this energy (ca. 67 keV).

### Nuclear reactions

When the proton beam interacts with the sample, two types of processes are of interest in this energy range:

1. There are those that result in X-ray emission, the char-

acteristic components of which can be used for analytical purposes.

2. There are nuclear reactions of the (p, xn) or (p, charged particle) type, that can result in the emission of  $\gamma$ -rays of discrete energy.

The nuclear reactions can be of two types, single stage or multistage. A single-stage reaction is a direct process: the emission of a  $\gamma$ -ray occurs simultaneously with the nuclear reaction. A multistage reaction normally results in the production of a compound system that decays to a more stable system through the emission of one particle (or more) or  $\gamma$ -rays over a period of time.

### $\gamma$ -ray interferences

It has been suggested that the interference of these discrete  $\gamma$ -rays with the X-ray spectrum is a serious problem in HE-PIXE work, sufficient to preclude its use as a viable analytical technique (Gerve and Schatz, 1975). The argument states that for a very complex material of unknown chemistry, a HE-PIXE spectrum may contain many X-ray and  $\gamma$  peaks, some of which may overlap, making the interpretation of line identities and the extraction of line intensities intractable. This may or may not be the case in an analysis. It does not however indicate any intrinsic deficiency in HE-PIXE, nor does it mean that HE-PIXE is any more or less intractable than many other analytical techniques. Alternatively, the same analytical use could be made of  $\gamma$ -rays in HE-PIXE as in nuclear reaction analysis (NRA), instrumental neutron activation analysis (INAA) or proton induced gamma emission (PIGE).

When analyzing geological materials, several techniques are usually required to adequately characterize the material (Calas and Hawthorne, 1988). Thus PIXE should not be used to analyze materials of unknown chemistry; it should be used to analyze for specific elements that are difficult to analyze by more conventional techniques in materials in which the composition and minerals have been well characterized by other methods. Knowledge of the mineral assemblage and major- and minor-element chemistry of a sample will usually provide sufficient constraints to allow a unique interpretation of the resulting spectrum.

X-ray lines are easily distinguished from  $\gamma$ -ray peaks by the fact that they are present in a spectrum as doublets or quadruplets, as opposed to single isolated lines. This distinguishing characteristic, along with the operating principles that (1) samples should be well characterized in terms of major-element chemistry and mineralogy, and (2) the PIXE experiment should be used to answer specific questions (it is not a general analytical method for preliminary characterization), suggests that HE-PIXE should be as applicable to mineral analysis as any other analytical technique.

### Trout Lake spectrum

In the Trout Lake spectrum (Fig. 2), the discrete  $\gamma$ -ray transitions present may be identified using constraints de-

rived from the sample minerals, together with the nuclear properties of the isotopes in the sample. Careful petrographic examination showed the presence of pyrite, chalcopyrite, sphalerite, quartz, and electrum. This restricts the initial species in any nuclear reaction process to the isotopes of Fe, S, Cu, Zn, Si, O, Au, Ag, and Hg.

The origin of the discrete  $\gamma$ -ray peak may be further constrained by estimating the half-life of the decaying isotope. To estimate the half-life, the target was first irradiated for 1 h at 40 MeV. The proton beam was then turned off, and a spectrum was recorded for 1 h. The counter was reset and a second spectrum recorded overnight. From the relative 67 keV peak intensities in the two spectra (corrected for different acquisition times), the half-life was determined to be on the order of a few hours.

Knowing that the  $\gamma$ -ray energy of interest was 67 keV, and the half-life of the decay was on the order of hours, together with the compositional constraints imposed by the minerals, it was possible to identify the reaction and the element giving rise to the observed  $\gamma$ -ray.

The  $\gamma$ -rays with energies in the region of 67 keV could be derived from  $^{61}\text{Cu}$ ,  $^{61}\text{Co}$ ,  $^{183}\text{Os}$ , and  $^{73}\text{Se}$  (Reuss and Westmeier, 1983). As indicated above, the observed minerals restrict the initial species in any nuclear reaction to the isotopes of Fe, S, Cu, Zn, Si, O, Au, Ag, and Hg. The only correspondence between the lists is Cu, and  $^{61}\text{Cu}$  is not a naturally occurring isotope. In fact none of these isotopes occur naturally. Production of  $^{61}\text{Co}$ ,  $^{183}\text{Os}$ , and  $^{73}\text{Se}$  cannot result from any 20–50 MeV proton-induced reaction involving any of the elements listed above. On this basis, we focused our attention on the  $^{61}\text{Cu}$  isotope. A (p, xn) reaction resulting in the production of a Cu isotope would have to involve Ni. This is considered to be unlikely for two reasons. First, Ni is present in the sample in only trace amounts (Healy and Petruk, 1988). Second, the isotope of Cu in which we are interested,  $^{61}\text{Cu}$ , cannot be produced by any (p, xn) reaction with 40 MeV protons for which the reaction cross section is high. By discounting Ni as the starting point for this reaction, any simple single-stage nuclear reaction is precluded, giving rise to the observed  $\gamma$ -ray; this means that multistage processes must be considered.

It is possible to produce an excited state of Cu ( $^{61}\text{Cu}^*$ ) by a (p,  $\alpha$ ) reaction with 40-MeV protons incident on  $^{64}\text{Zn}$  (Guazonni et al., 1976). The  $^{61}\text{Cu}^*$  will then decay to the ground state of  $^{61}\text{Cu}$  ( $^{61}\text{Cu}_{gs}$ ) by the emission of a 67-keV  $\gamma$ -ray; the half-life of this reaction is 3.37 h, in agreement with our initial estimate on the order of a few hours.

To test this identification, a reference Zn foil was irradiated with 40-MeV protons; a specimen of sphalerite (ZnS) was also irradiated to constrain any possible mineralogical influences. As seen in Figure 3, the Zn foil has a strong peak at 67 keV; this peak was also observed in the sphalerite spectrum. This peak overlaps almost exactly with the  $\text{Au}K\alpha_2$  peak. Thus, the  $\text{Au}K\alpha_1/K\alpha_2$  intensity ratio observed in the Trout Lake sample is due to the production of an excited state of Cu ( $^{61}\text{Cu}^*$ ) by a (p,  $\alpha$ ) reaction with  $^{64}\text{Zn}$  (the most abundant natural isotope of Zn), followed by  $^{61}\text{Cu}^*$  decay by the emission of a 67-keV

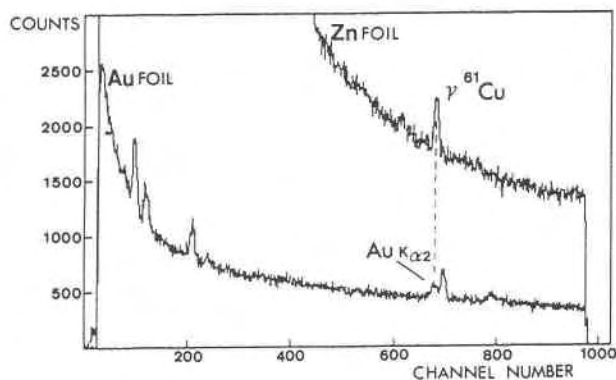


Fig. 3. Spectra from Zn foil and Au foil showing the overlap that occurs between the  $\text{Au}K\alpha_2$  X-ray line and the  $\gamma$ -ray produced as a result of  $^{61}\text{Cu}$  decay.

$\gamma$ -ray. The initial Zn was present as sphalerite in the sample.

## DISCUSSION

Accelerator-based analytical systems are being applied to geochemical problems where trace, in situ, microscale analysis is required. As it has been applied to a specific problem, each technique has presented new difficulties, some technical and related to the physics involved and the material analyzed, and some of a more specific geochemical nature when geochemically coherent elements are being analyzed. HE-PIXE is no exception, but it also offers some new and important avenues of investigation.

### HE-PIXE of Au

Having identified each component in the Trout Lake spectrum, we can consider the analytical strategy necessary for this type of material. First, it is possible to vary the incident beam energy; the MA-HEM system (McKee et al., 1990) is variable between 20 and 50 MeV such that the production of discrete  $\gamma$ -ray emitting nuclei is minimized. This was not feasible for the Trout Lake sample, as the cross section for the  $^{61}\text{Cu}$ -producing reaction does not vary significantly between 20 and 40 MeV (Guazonni et al., 1976). However, this possibility may be useful with other discrete  $\gamma$ -ray interferences.

One additional complication occurs in the study of Au-bearing samples. A (p, n) reaction on Au will generate trace amounts of Hg (cf. Ramsay et al., 1978), which will in turn produce K X-ray when irradiated by the proton beam. These will be detected and will accumulate in the spectrum as normal X-ray peaks. However, as the cross section for this reaction is known, the amount of Hg produced over and above what was originally in the sample can be easily determined.

### HE-PIXE, LE-PIXE, and SXRF

The combination of energy-dispersive spectrometers with proton accelerators has allowed simultaneous multi-element analysis using LE-PIXE since the early 70s. (Cahill, 1980). LE- $\mu$ -PIXE has been applied to a number of

mineralogical problems as the methodology and technology have matured. Lower limits of detection depend on the resolution of a signal above background, and detection limits range from 5 to 30 ppm for elements with  $Z$  from 30 to 55 (Campbell et al., 1990).

In all forms of X-ray analysis, including thick-target LE-PIXE ( $E_p = 2\text{--}5$  MeV), the X-ray signal is a function of the ionization cross section for the  $K$ ,  $L$ , and  $M$  electron shells. For low-energy protons, the cross section is high for the  $K$  shells of light elements and the  $L$  shells of heavy elements, providing sufficient fluorescent yield for analytical purposes. For heavy elements ( $Z > 55$ ), low-energy protons cannot ionize  $K$ -shell electrons and analysis depends on the use of  $L$  X-ray lines. Such  $L$  X-ray spectra are complex and can be affected by overlapping  $K$  X-rays from lighter elements (cf. Campbell et al., 1990). Both spectral overlap and complexity can lead to difficulties and ambiguity in the interpretation of  $L$ -line spectra, a problem that is exacerbated by uncertainty in relative  $L$  X-ray line intensities. In thick-target LE-PIXE, the proton beam is stopped by the sample, producing significant background radiation from proton scattering and matrix effects; this can obscure X-ray signals from elements present in low concentrations. LE-PIXE probes can provide in situ analysis with spatial resolution of about  $5\ \mu\text{m}$  (significantly better than what is presently, and routinely, available with HE-PIXE), and lower limits of detection are about 30 times lower than that obtained by electron probe microanalysis (EPMA). LE-PIXE is ideal for the analysis of light trace elements ( $Z < 55$ ) using  $K$  X-ray lines.

HE-PIXE is a new technique; it has only recently been applied to geological materials (Durocher et al., 1988), and instrumentation, sample-preparation, and sample-handling techniques are still being developed. Analytical precision and lower limits of detection in HE-PIXE will depend upon such factors as the material being analyzed, sample preparation (e.g., uniformity of sample thickness and polish), exposure time, beam current, and the stability of the magnetic field controlling the beam. Transmission targets of the type used in this experiment have the advantage of being essentially transparent to the proton beam; thus there are virtually no matrix effects (sample heating is also negligible), and signal-to-noise ratios are inherently high. In HE-PIXE the fluorescent yields for  $K$  X-rays of heavy elements are high. The relationship between  $K$ -shell ionization cross section,  $K$ -shell electron binding energy, and the energy of incident protons in HE-PIXE has been described by McKee et al. (1976). The cross section for  $K$ -shell ionization in heavy elements reaches a maximum at approximately 40 MeV because of the similarity in the incident proton velocity to the electron orbital velocity in  $K$  shells of heavy elements.  $K$  X-ray spectra for heavy elements are comparatively simple and are less subject to complex interferences. All these features are advantageous when analyzing trace quantities of heavy elements in geochemically complex samples.

McKee et al. (1981) and Durocher et al. (1988) have

shown that detection limits for HE-PIXE analysis of heavy elements are typically on the order of a few ppm. Peisach and Pineda (1989) have suggested that detection limits on the order of 20 ppb can be achieved. For heavy elements,  $K$  X-ray fluorescent yields (which are related to the  $K$ -shell ionization cross sections) are relatively constant with respect to atomic number for excitation by 40-MeV protons (McKee et al., 1976); consequently sensitivity should be fairly constant for heavy elements. Detection limits for the experiments in this study are on the order of 2–10 ppm but are capable of significant improvement.

SXRF microprobes have been used for geochemical analysis utilizing the  $K$  X-ray lines for rare-earth elements (Chen et al., 1990) and As, Se, Pd, Ru, and Sn in sulfide minerals (Cabri et al., 1985b). Spatial resolution of  $10\ \mu\text{m}$  is possible, comparable with low-energy PIXE ( $5\ \mu\text{m}$ , Campbell et al., 1990) and HE-PIXE ( $10\text{-}\mu\text{m}$  spot sizes are possible, McKee et al., 1990). Minimum detection limits of 1–10 ppm are practical (Chen et al., 1990), and these levels can be achieved with very short analytical times (a few seconds). Limits in the ppb range are theoretically possible with present technology (Chen et al., 1990; Rivers et al., 1987, 1988). SXRF has the advantage of achieving these very low detection limits while delivering energy to the sample that is less by orders of magnitude than EPMA and PIXE (Chen et al., 1990); therefore where damage to a sample is a potential constraint upon the analysis, SXRF would be the method of choice.

#### Combined HE-PIXE HE-PIGE analysis

The  $\gamma$ -ray from the electrum sample is essentially the product of a nuclear reaction that creates a compound system. NRA and PIGE of geological materials has been restricted to light isotopic systems as a function of low beam energies (cf. Sutton et al., 1988; Cole and Ohmoto, 1986; Smith et al., 1985). In principle, with higher and variable energies (depending on the accelerator used) and knowledge of the cross section of nuclear reactions, heavy trace-element analysis and heavy isotope analysis may be possible by HE-PIGE.

HE-PIGE and NRA may be applied to the analysis of geochemically coherent elements where HE-PIXE by itself is not ideal. Trace amounts of a heavy element should be detectable by means of the PIGE spectrum when the corresponding  $K$  X-ray signal is too weak or is obscured by more intense X-ray lines of geochemically coherent elements (e.g., Pt in the presence of Os and Ir).

#### Isotopic systems

The important point about PIGE is that it is a nuclear reaction technique, and as such is an isotopic probe. If we reverse our argument (from the HE-PIXE case), we can maximize the signal from the  $\gamma$ -ray and use it to analyze for the relevant isotope. In the Trout Lake sample, the ( $p, \alpha$ ) reaction involved an isotope of Zn ( $^{64}\text{Zn}$ ), and thus the intensity of the resulting  $\gamma$ -ray (from the decay of  $^{61}\text{Cu} \rightarrow ^{61}\text{Cu}_{\beta\beta}$ ) is a measure of the abundance of

$^{64}\text{Zn}$ . This indicates the potential of HE-PIGE for microprobe isotopic analysis. For example,  $^{34}\text{S}/^{32}\text{S}$  ratios are of considerable geological interest. A (p, n) reaction with  $^{32}\text{S}$  produces  $^{32}\text{Cl}$ , which decays by the emission of  $\gamma$ -rays with energies of 2.23 and 4.77 MeV. A (p, n) reaction with  $^{34}\text{S}$  produces  $^{34}\text{Cl}$ , which decays by the emission of a 2.12-MeV  $\gamma$ -ray. In such a case, a high-energy  $\gamma$ -ray detector would be required, and the intensity of the  $\gamma$ -rays will be a function of the cross section for the (p, n) reactions and the concentration of the isotope. Thus, in principle, it should be possible to do microscale in situ isotopic analysis using HE-PIGE.

### CONCLUSIONS

HE-PIXE has the potential for analysis of trace elements in sulfide minerals. Working at these higher energies produces *K*-line spectra for even the heaviest elements (Halden, 1990; Halden et al., 1990). In the present case, even though  $\text{AuK}\alpha_1$  overlaps with  $\text{HgK}\alpha_2$ , there is no interference with the  $\text{HgK}\alpha_1$  peak, and thus the  $\text{HgK}\alpha_2$  interference may be stripped out, leaving the  $\text{AuK}\alpha_1$  peak without overlap. These problems are no more involved (often less so) than current treatment of major elements using EDS in electron microprobe analysis.

To interpret HE-PIXE spectra, the analyst must have a knowledge of the deexcitation processes that create X-rays and the nuclear processes and reactions that can create  $\gamma$ -rays. Discrete  $\gamma$ -ray interferences do occur, but these may be identified from the mineralogical and geochemical characteristics of the sample and distinguished from X-ray lines. Nuclear and X-ray data tables (e.g., Reuss and Westmeier, 1983) and knowledge of the nuclear cross sections for various reactions (in this case proton reactions) will allow prediction of what analytical lines (X-ray or  $\gamma$ -ray) are to be expected in an energy region of interest. Resolution of the individual *K* $\alpha$  and *K* $\beta$  lines should usually give at least one intense line for analytical purposes. This work suggests that, although much still remains to be explored, HE-PIXE should eventually be a useful addition to the techniques used in mineral analysis.

### ACKNOWLEDGMENTS

We wish to thank both the reviewers and particularly Associate Editor Glenn Waychunas for comments that materially improved the paper. We thank R.A. Healy for the Trout Lake sample, L.A. Groat for technical assistance and G.S. Clark for reviewing the manuscript. This work was supported by NSERC operating grants OGP0000612 to N.M.H., OGP0000806 to F.C.H. and OGP0003256 to J.S.C. McK. and by NSERC infrastructure grant no. INF0005302.

### REFERENCES CITED

- Cabri, L.J. (1987) The mineralogy of precious metals: New developments and metallurgical implications. *Canadian Mineralogist*, 25, 1–7.
- Cabri, L.J., Blank, H., El Gorsej, A., LaFlamme, J.H.G., Nobiling, R., Sizgoric, M.B., and Traxel, K. (1984) Quantitative trace-element analysis of sulfides from Sudbury and Stillwater by proton microprobe. *Canadian Mineralogist*, 22, 521–542.
- Cabri, L.J., Campbell, J.L., LaFlamme, J.H.G., Leigh, R.G., Maxwell, J.A., and Scot, J.D. (1985a) Proton-microprobe analysis of trace elements in sulfides from some massive-sulfide ore deposits. *Canadian Mineralogist*, 23, 133–148.
- Cabri, L.J., Rivers, M.L., Smith, J.V., and Jones, K.W. (1985b) Trace elements in sulphide minerals by milliprobe X-ray fluorescence using white synchrotron radiation (abs.). *EOS*, 66, 1150.
- Cahill, T.A. (1980) Proton microprobes and particle induced X-ray analytical systems. *Annual Review of Nuclear and Particle Science*, 30, 211–252.
- Calas, G., and Hawthorne, F.C. (1988) Introduction to spectroscopic methods. *Mineralogical Society of America Reviews in Mineralogy*, 18, 1–9.
- Campbell, J.L., Cabri, L.J., Rogers, P.S.Z., Traxel, K., and Benjamin, T.M. (1987) Calibration of micro-PIXE analysis of sulfide minerals. In J.W. Nelson, Ed., *Proceedings of the 4th International Conference on PIXE and its Analytical Applications*. *Nuclear Instruments and Methods*, B22, 437–441.
- Campbell, J.L., Maxwell, J.A., Teesdale, W.J., Wang, J.-X., and Cabris, L.J. (1990) Micro-PIXE as a complement to electron probe microanalysis in mineralogy. *Nuclear Instruments and Methods in Physics Research*, B44, 347–356.
- Chen, J.R., Chao, E.C.T., Minkin, J.A., Back, J.M., Jones, K.W., Rivers, M.L., and Sutton, S.R. (1990) The uses of synchrotron radiation sources for elemental and chemical microanalysis. 5th International Conference on Particle Induced X-ray Emission and its Analytical Applications. Amsterdam, August 21–25, 1989, Programme and Abstracts.
- Cole, D.R., and Ohmoto, H. (1986) Kinetics of isotopic exchange at elevated temperatures and pressures. *Mineralogical Society of America Reviews in Mineralogy*, 16, 41–90.
- Cookson, J.A. (1979) The production and use of a nuclear microprobe of ions at MeV energies. *Nuclear Instruments and Methods*, 165, 477–508.
- (1981) The use of the PIXE technique with nuclear microprobes. *Nuclear Instruments and Methods*, 181, 115–124.
- Durocher, J.J.G., Halden, N.M., Hawthorne, F.C., and McKee, J.S.C. (1988) PIXE and micro-PIXE analysis of minerals at  $E_p = 40$  MeV. *Nuclear Instruments and Methods*, B30, 470–473.
- Folkman, F., Gaarde, C., Huus, T., and Kemp, K. (1974) Proton induced X-ray emission as a tool for trace-element analysis. *Nuclear Instruments and Methods*, 116, 487–499.
- Gerve, A., and Schatz, G. (1975) Applications of cyclotrons in technical and analytical studies. In W. Joho, Ed., *Proceedings 7th International Conference on Cyclotrons and their Applications*, p. 496–502. Birkhauser, Basel.
- Gould, C.R., Holzweig, L.G., King, S.E., Lau, Y.C., Poore, R.V., Robertson, N.R., and Wender, S.A. (1981) The XSYS data acquisition system at Triangle Universities Nuclear Laboratory. *IEEE Transactions on Nuclear Science*, NS-28, 3708–3714.
- Guazzoni, P., Pignaneli, M., Colombo, E., and Crescentini, F. (1976) Energy dependence of transfer reactions on  $^{64}\text{Zn}$  and two step processes. *Physics Reviews*, C13, 1424–1433.
- Halden, N.M. (1990) High-energy PIXE of heavy elements in geological materials. *International Mineralogical Association Abstracts with Program*, Beijing, June 30–July 3, 435–436.
- Halden, N.M., Hawthorne, F.C., Durocher, J.J.G., McKee, J.S.C., and Mirzai, A. (1990) High-energy Platinum and other element PIXE. *Geological Association of Canada/Mineralogical Association of Canada Annual Meeting Abstracts with Program*, Vancouver, May 16–18, p. 52.
- Healy, R.A., and Petruk, W. (1988) Compositional and textural variation in Au-Ag-Hg alloy from the Trout Lake deposit, Flin Flon, Manitoba. *Canmet report MRP/MSL 88-49 (J)*, Department of Energy, Mines and Resources, Canada.
- MacArthur, J.D., Ma, X.P., Anderson, A.J., and Černý, P. (1987) PIXE analysis of apatites from granitic pegmatite dikes near Cross-Lake Manitoba. In J.D. Brown and R.H. Packwood, Eds., 11th International Congress on X-ray Optics and Microanalysis, p. 175–180, London.
- McKee, J.S.C., Randell, C.P., and Wilk, S.F.J. (1976) Proton induced X-ray analysis of heavy elements as an environmental probe. In E. O'Mongain and C.P. O'Toole, Eds., *Physics in industry*, p. 183–186. Pergamon Press, New York.
- McKee, J.S.C., Lapointe, C., Birchall, J., Pinsky, C., and Bose, R. (1981)

- Analysis of cesium in tissue samples using the PIXE technique. *Journal of Environmental Science and Health*, A16(5), p. 465–475.
- McKee, J.S.C., Durocher, J.J.G., Gallop, D., Halden, N.M., Mathur, M.S., Mirzai, A., Smith, G.S., and Yeo, Y.H. (1990) Micro- and milli-PIXE analysis at 40 MeV—Why, how and when? *Nuclear Instruments and Methods in Physics Research*, B45, 513–515.
- Peisach, M., and Pineda, C.A. (1989) *K* X-ray production from rare earths by high energy protons. 5th International Conference on Particle Induced X-ray Emission and its Analytical Applications. Amsterdam, August 21–25 1989, Programme and Abstracts, 103.
- Ramsay, W.D., Al-Ghazi, M.S.A.L., Birchall, J., and McKee, J.S.C. (1978) Atomic *K*-shell ionization induced by 20–50 MeV protons. *Physics Letters*, 69A, 258.
- Reuss, U., and Westmeier, W. (1983) Catalog of gamma rays from radioactive decay, Part II. Atomic data and nuclear data tables 29, 2.
- Rivers, M.L., Sutton, S.R., Smith, J.V., and Jones, K.W. (1987) Synchrotron X-ray fluorescence microprobe. I. Theory, experimental techniques, and analytical procedure. *Geological Society of America Abstracts with Programs*, 821.
- Rivers, M.L., Sutton, S.R., and Smith, J.V. (1988) The advanced photon source, a national facility for the geosciences: Technical capabilities (abs.). *EOS*, 69, 504.
- Rogers, P.S.Z., Duffy, C.J., Benjamin, T.M., and Maggiore, C.J. (1984) Geochemical applications of nuclear microprobes. *Nuclear Instruments and Methods*, B3, 671–676.
- Scofield, J.H. (1974) Exchange corrections of *K* X-ray emission rates. *Physics Reviews*, A9, 1041–1049.
- Smith, J.V., Skirius, C.M., Rivers, M.L., and Jones, K.W. (1985) Optical and trace-element signatures of quartz as indicators of crystallization conditions (abs.). *EOS*, 66, 1117.
- Sutton, S.R., Smith, J.V., Jones, K.W., and Dawson, J.B. (1988) Nitrogen in the Earth: Progress in development of the  $^{14}\text{N}(d, \alpha)^{12}\text{C}$  microprobe technique (abs.). *EOS*, 69, 502.
- Waychunas, G.A. (1988) Luminescence, X-ray emission and new spectroscopies. *Mineralogical Society of America Reviews in Mineralogy*, 18, 639–698.

MANUSCRIPT RECEIVED JUNE 23, 1989

MANUSCRIPT ACCEPTED JULY 25, 1990